Takashi Mitsuda
mitsuda@md.okayama-u.ac.jp
Faculty of Health Sciences
Okayama University Medical School
2-5-1 Shikata-cho, OKAYAMA
700-8558 JAPAN

Sachiko Kuge
SHARP Corporation

Masato Wakabayashi
Department of Robotics
Ritsumeikan University

Sadao Kawamura
Department of Robotics
Ritsumeikan University

Wearable Force Display Using a Particle Mechanical Constraint

Abstract

A particle mechanical constraint (PMC) is a soft vinyl tube containing Styrofoam beads. It can be freely compressed, elongated, bent, twisted, or otherwise manipulated in all degrees of freedom. Evacuation of the air inside the tube makes the PMC rigid so that it maintains whatever shape it has been given. The stiffness of the PMC is proportional to the reduction in internal pressure below atmospheric pressure. Viscosity is also controlled virtually by changing the inside air pressure in proportion to the speed of transformation of the PMC. We used a PMC to develop a wearable force display that provides the sensation of coming into contact with a wall or of moving in water with viscosity, in addition to that of moving in air. PMC is an inherently passive device that never exerts excessive force if it were to malfunction. In short, it is suitable as a wearable human interface because it is light, soft, and safe.

1 Introduction

A force display generally requires an actuator that exerts a force on the human body. Examples of such actuators include a robot arm (Brooks, Young, Batter, & Kilpatrick, 1990; Kazerooni & Guo, 1993; Bergamasco et al., 1994), a wire system driven by a servo motor (Ishii & Sato, 1994; Kawamura, Ida, Wada, & Wu, 1995) and a pneumatic cylinder (Burdea, Zhuang, Roskos, Deborah, & Langrana, 1992). These systems carry a risk of exerting excessive force accidentally, and these wearable interfaces could be lethal to the user if they were to malfunction. To overcome this problem, devices that exert a force in a passive way have been investigated. Sakaguchi, Fukusumi, and Furusho (2000) developed a passive force display using a manipulandum with ER brakes. This system provides a reaction force to the hand via the braking torque of the manipulandum. Colgate (1996) developed a passive force display using nonholonomic joints. This system exerts a reaction force to the hand through a handle with a wheel that rotates against the direction of movement. Because these systems do not create any power by themselves, they are intrinsically safe. However, it is difficult to increase the degrees of freedom of such systems while suppressing their weight and size.

In the present study, we examined a novel passive device called a *particle mechanical constraint,* which consists of Styrofoam beads and vinyl films, making it lighter and softer than previous passive devices. It is driven by vacuum pressure, and so it is safer than electric devices when broken. Aldridge, Carr, England, Meech, and Solomonides (1996) developed a similar passive device that, using an amorphous blob filled with fine particles, provides the sensation

Presence, *Vol. 11, No. 6, December 2002,* 569–577

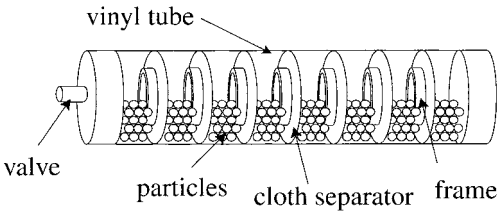

Figure 1. *Structure of a PMC.*

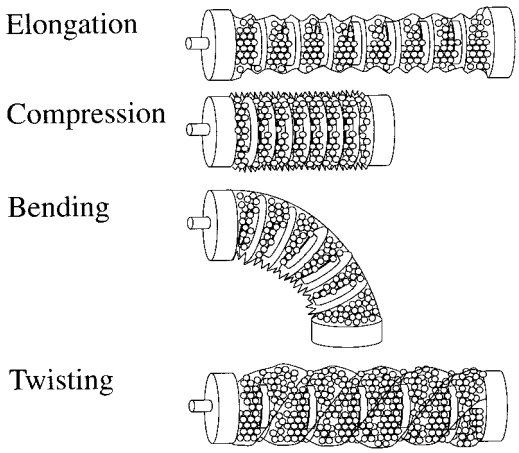

Figure 2. *Various transformations of a PMC.*

of grasping an object. PMC's advantage compared with this amorphous passive device is that the PMC internal structure enables it to be compressed, elongated, bent, or twisted without a loss in stiffness. The stiffness of the PMC is proportional to the reduction in internal pressure below atmospheric pressure. The viscosity can be controlled by changing the inside air pressure according to the speed at which the PMC is deformed. We describe the control methods and experimental results of the application as a wearable force display.

2 The Structure of the PMC

Figure 1 depicts the structure of the PMC. Styrofoam beads are enveloped in a vinyl chloride tube. Two resin frames, one at each end of the PMC, maintain the tubular shape. The PMC is airtight, and the inside air moves only through a valve at one end. When the valve is open, the PMC is soft and its shape can be changed easily because the inside air and the embedded particles can move freely. Figure 2 depicts various manipulations of the PMC, such as elongation, compression, bending, and twisting. When the inside air is evacuated via the valve connected to a vacuum pump, atmospheric pressure compresses the PMC and the embedded particles solidify cohesively. The stiffness of the PMC increases as internal pressure decreases below atmospheric pressure. To ensure that particles are distributed uniformly regardless of how the PMC is reshaped or manipulated, the area inside the tube is divided into several compartments. These compartments are separated by cloth discs that allow ventilation. In addition, a resin ring, serving as a frame, is fixed concentrically to each disc to prevent deep wrinkles from forming in the film that covers the tube. (Such wrinkles would decrease the stiffness of the PMC.) The diameter of these frames is less than the inner diameter of the PMC. If the frames were to have the same diameter as the PMC, no wrinkles along the long axis of the element would appear, and then wrinkles along the circumference would shorten the PMC. Controlling the amount of embedded particles is important to determine the range of transformation. An increase in the number of particles usually makes the PMC harder. However, it also decreases the range of possible transformation of the PMC. Moderate amounts of particles are necessary to prevent deep wrinkles of the covering film. The moderate ratio of the amount of particles to the capacity of the PMC is approximately 50% to 70%, according to our experience. The basic characteristics of the PMC are as follows.

- It is soft. It can be compressed, elongated, bent, and twisted freely.
- The stiffness is proportional to the decrease in internal pressure below atmospheric pressure.
- It is lightweight, as it consists of only Styrofoam beads and vinyl tubing.
- It is safe when broken, because it operates by vacuum pressure.
- It can be formed into arbitrary shapes as desired.

3 Mechanical Properties of the PMC

This section describes the mechanical properties of the PMC and the effect of the inside vacuum pressure.

3.1 Structure

We measured the mechanical properties of a PMC. The PMC used in this experiment was 200 mm long, had an outer diameter of 90 mm, and weighed 80 g. The covering film was 0.1 mm thick. The diameter and the weight of each particle were 2 mm and 0.06 g/cm^3, respectively. The inside of the PMC was divided into four chambers of equal length by discs of soft cloth. The tube was filled to 50% of its capacity with the embedded particles.

3.2 Range of Transformation

Figure 2 depicts some transformations of the PMC used in this study. The minimum length of the PMC was 100 mm. The length (the maximum compression) depends on the amount of embedded particles. The maximum length of the PMC was 170 mm, which was shorter than the length of the film; the evacuation of air created wrinkles on the covering film, thereby shortening the PMC by 30 mm. When the initial length of the PMC was 170 mm, the evacuation and resultant wrinkling caused a 10 mm shortening. When the initial length was 150 mm or 130 mm, the shortened length was 5 mm or 2 mm, respectively. The maximum bending angle and twisting angle were 120 deg. and 90 deg., respectively. These angles depended also on the number of embedded particles.

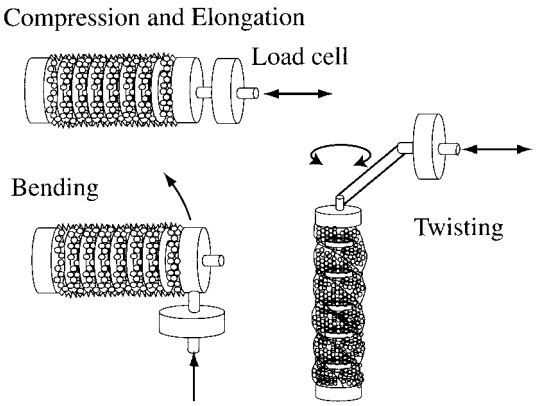

Figure 3. *Experimental setup.*

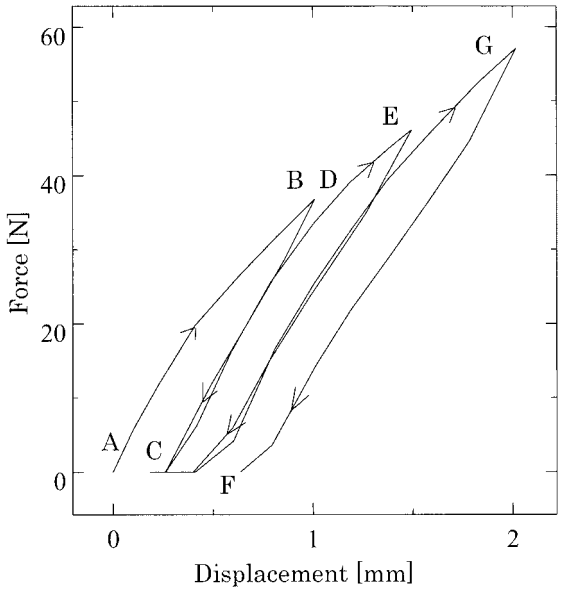

Figure 4. *Stiffness in compression.*

3.3 Basic Mechanical Properties

We measured the static mechanical properties using the experimental setup depicted in figure 3. In all measurements, the load was placed on the edge of the PMC, and the displacement and the reaction force were measured simultaneously. The particles were "fluffed up" before the measurements so that they would be distributed uniformly. The displacement was repeated several times continuously without additional fluffing of the particles. Figure 4 shows the relation between the displacement and the reaction force during compression. The initial length of the PMC was 170 mm after the air was evacuated, and the inside air pressure was −80 kPa. The relation between the reaction force and the displacement formed a gentle curve during the first compression (from A to B), but the relation during the elongation (B to C) was straight, and a permanent set of

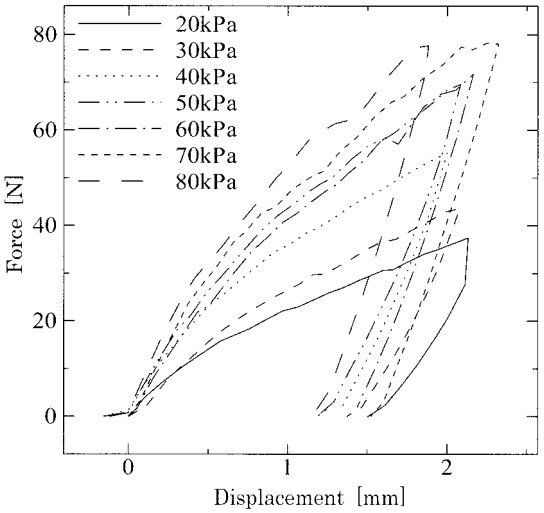

Figure 5. *Stiffness as a function of internal pressure.*

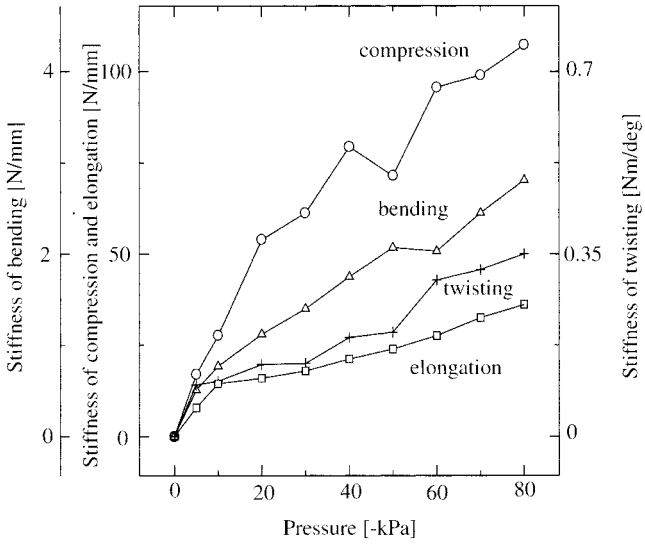

Figure 6. *Stiffness for different modes (bending, twisting, and so on) as a function of internal pressure.*

distortion remained. The relation during the second compression was also straight at the beginning (C to D), but then it drew a gentle curve again when the displacement exceeded the maximum displacement applied before (D to E). This hysteresis also appeared in the elongation, bending, and twisting displacements. We called the stiffness at the first loading the *initial stiffness* and the stiffness upon the following loading the *repeated stiffness.*

3.4 Effect of Inside Air Pressure

Figure 5 shows the levels of stiffness resulting from compression at various inside air pressures. This figure presents the change in stiffness from the first compression to the following elongation. For compression and elongation, as well as for bending and twisting, the stiffness was proportional to the reduction in internal pressure below atmospheric pressure. Figure 6 presents the relations between the repeated stiffness and the inside air pressure during compression, bending, twisting, and elongation. In all cases, stiffness was proportional to the inside vacuum pressure. The elongation stiffness was measured when the PMC was compressed to 100 mm. The bending stiffness and the twisting stiffness were measured when the length of the PMC was

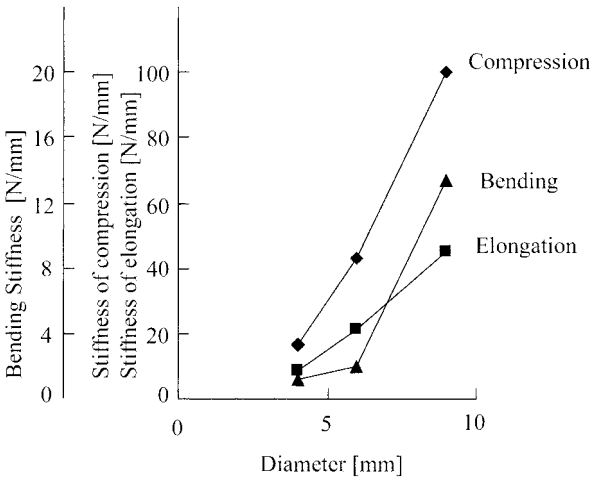

Figure 7. *Effect of diameter on the initial stiffness.*

170 mm. The initial stiffness was also proportional to the inside vacuum pressure.

3.5 Effect of the PMC Diameter

The characteristics of the PMC are different from the beam theory in the study of material dynamics. Figure 7 shows the relation between the diameter of the PMC and the stiffness in compression, elongation, and

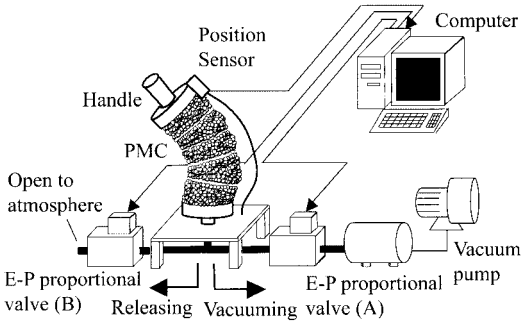

Figure 8. *Haptic display system.*

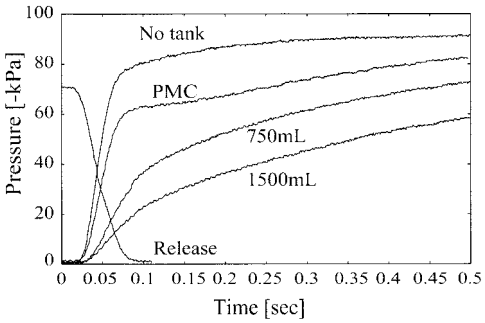

Figure 9. *Step responses of several designs.*

bending. The beam theory describes that the stiffnesses of compression and elongation are proportional to the section area. In contrast, the stiffness of compression of the PMC was proportional to a value between the diameter and the section area. The stiffness of elongation was proportional to the diameter. The stiffness of bending was proportional to the second moment of area, which coincides with beam theory. We are investigating the mechanism underlying the stiffness of the PMC, but, because so many parameters must be measured (such as the mechanical properties of the particles and those of the vinyl film), this mechanism has not yet been clarified.

4 Control of Stiffness and Viscosity

We developed a force display that exerts the stiffness and viscosity by controlling the inside air pressure of the PMC. This section describes the control system and the experimental results.

4.1 Control System

Figure 8 represents a schematic structure of the force display. The length of the PMC used in this experiment was 600 mm, and the outer diameter was 90 mm. The bottom end of the PMC was affixed to a table, and the top end was connected to a handle for operation. The operator feels a reaction force at the handle. An electromagnetic sensor (Polhemus FASTRAK) was attached to the handle, and the position of the handle was measured through a computer at 120 Hz. The PMC was connected to two E-P proportional valves (VEP3141 flow control, SMC, Inc.) that each controlled a cross section area of the air tube by signals from the computer. A vacuum pump (DTP-180S, ULVAC, Inc.) evacuated the internal air of the PMC through E-P proportional valve A. Valve B, when opened, allowed air from the atmosphere into the PMC. The inside air pressure of the PMC was controlled by the ratio of the two cross-sectional areas. For example, when valve A was closed and valve B was open, the inside air pressure was at the atmospheric level. In contrast, when valve A was open and valve B was closed, the inside air pressure was the ultimate vacuum pressure.

4.2 Step Response

To examine the vacuum control of this system, we measured the step responses of the inside air pressure control in several conditions. Figure 9 presents the results. It took 0.1 sec. to decrease the air pressure in the PMC from the atmospheric level to −60 kPa. When the vacuum pump was not connected to a tank (that is, when the PMC was disconnected from the system), it took 0.05 sec. to decrease the air pressure from the atmospheric level to −60 kPa. The air pressure reached −80 kPa in 0.1 sec. The difference in the ultimate vacuum pressure between the two conditions was caused by air leaking from the PMC. Increasing the air pressure in the PMC from −70 kPa to the atmospheric level

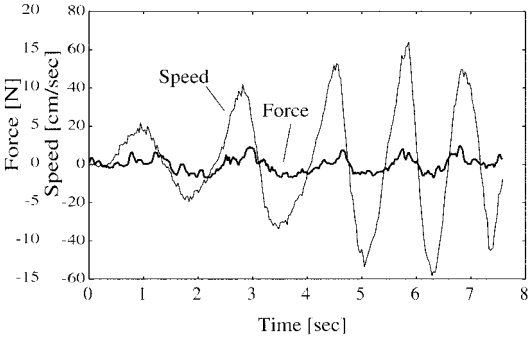

Figure 10. *Reaction force during no control.*

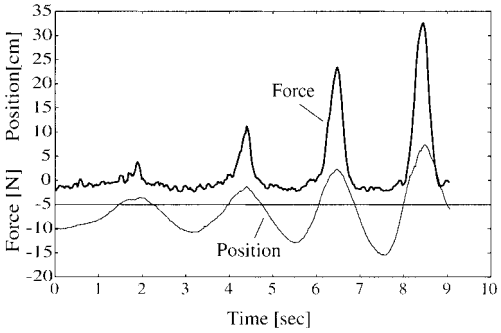

Figure 11. *Stiffness display.*

took 0.1 sec. When a 750 ml tank was connected to the system, it took 0.27 sec. to decrease the air pressure to −60 kPa. When a 1500 ml tank was connected, it took 0.55 sec. In all of the conditions, the air pressure started to change after 0.02 sec. Therefore, the latency of the valve control was 0.02 sec. The speed at which the air pressure was controlled depended on the air capacity of the object. Many other factors are involved in the evacuation speed, such as the power of the vacuum pump, the size and the length of the air tube, and the cross-sectional area of the valve. Improving these factors tends to increase the weight of the system. We are investigating ways to reduce the total weight of the system by modifying the hardware and the controlling scheme.

4.3 Stiffness Display

The stiffness of the PMC was controlled by changing the inside air pressure in proportion to the desired stiffness. Here we show an example in which the sensation of touching a wall is created by controlling the stiffness. To simplify the experiment, the operator pushed and pulled the handle successively on a horizontal line. Figure 10 presents the reaction force at the operator's hand when the stiffness of the PMC was set to the minimum (that is, when the inside air pressure of the PMC was set to the atmospheric level). The reaction force was less than 2 N. Figure 11 presents the reaction force when the stiffness of the PMC was set to the maximum (the inside air pressure of the PMC set to −70 kPa) when the handle crossed the virtual wall position (−5 cm). When the handle was pulled, the stiffness of the PMC was set to the minimum. As the figure shows, the reaction force increased rapidly when the position of the handle crossed −5 cm. This means that the operator perceived a sensation of touching the wall. By changing the stiffness of the PMC, the operator can perceive sensations of touching objects of various stiffnesses. Figure 12 presents the relations between the reaction force and the handle position when the inside air pressure was set to −10 kPa, −20 kPa, −40 kPa, and −70 kPa during the contact with the virtual wall.

4.4 Viscosity Display

Viscosity was exerted by controlling the inside air pressure in proportion to the speed of the handle. In this way, the operator was able to perceive the sensation of moving his or her hand through water. Figure 13 presents the reaction force and the handle speed when the operator pushed and pulled the handle successively at various speeds. The inside air pressure P[kPa] was set to $-V/2$, where V[cm/sec.] was the handle speed. This figure shows how the reaction force changed in proportion to the handle speed, although a small delay was observed. The viscosity can be controlled by changing the ratio between the inside air pressure and the handle speed. Figure 14 presents the relation between the reaction force and the handle speed when the inside air pressure was set to $-V/8$, $-V/4$, $-V/2$, or $-V$.

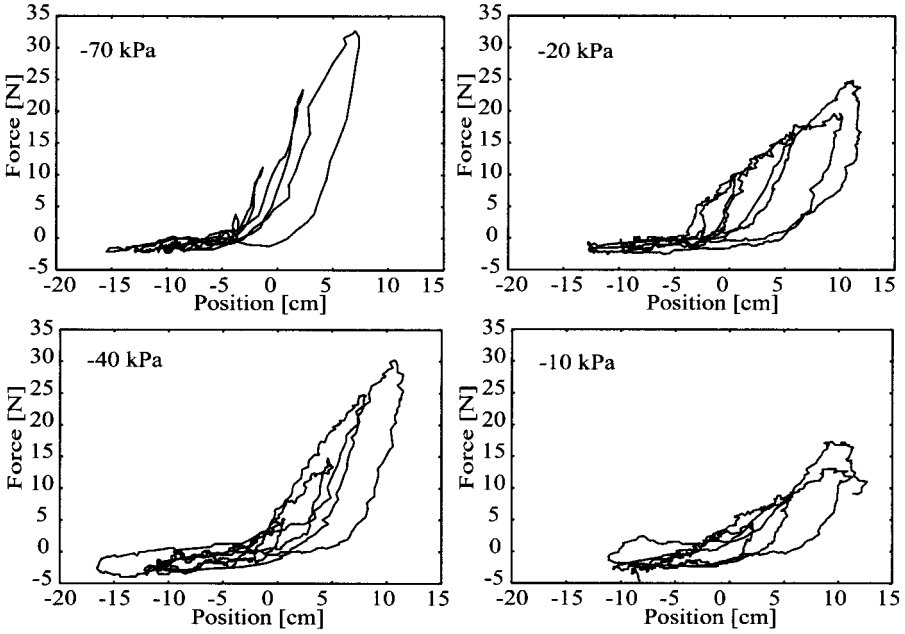

Figure 12. *Relation between position and reaction force in four different vacuum pressures.*

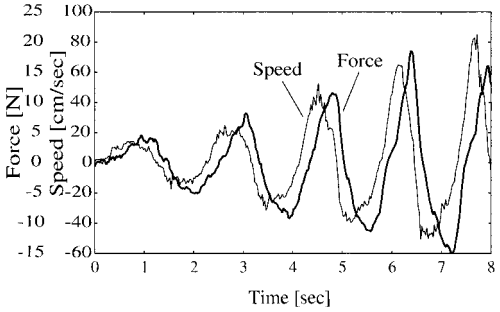

Figure 13. *Viscosity display.*

5 Wearable Force Display

We developed the wearable force display depicted in figure 15. One end of a PMC was fixed to the underarm of the operator, and the other end was attached to a glove. The operator handled the glove and perceives the viscosity and elasticity by the method described previously. Although the weight of the PMC was 250 g, the operator did not feel the weight because the bulk of the PMC was attached to the underarm and was therefore supported by the trunk rather than the arm.

Figure 16 depicts the virtual haptic environment that was used for the experiments. An operator moving the glove in this environment can feel three types of sensation: the sensation of moving his or her hand in the air without any reaction force, the sensation of moving the hand in water with viscosity, and the sensation of touching a wall. Figure 17 shows an experimental result in which the operator first moved the glove in air, then moved it through water, changing the speed of movement in order to feel the sensation of viscosity, and finally reached the wall. The hand position, the hand speed, and the reaction force in these three virtual environments are shown in the figure. The reaction force in air was almost zero, and it was proportional to the speed in water. When the hand arrived at the wall position, the reaction force increased rapidly and provided a sensation of touching. Because there was a small latency in the vacuum control, there was a brief delay before the operator felt the touching sensation when moving the hand at high speed. Reducing this latency will be an important task in the future to enable this system to display force with quicker motions.

The biggest merit of this system is its light weight,

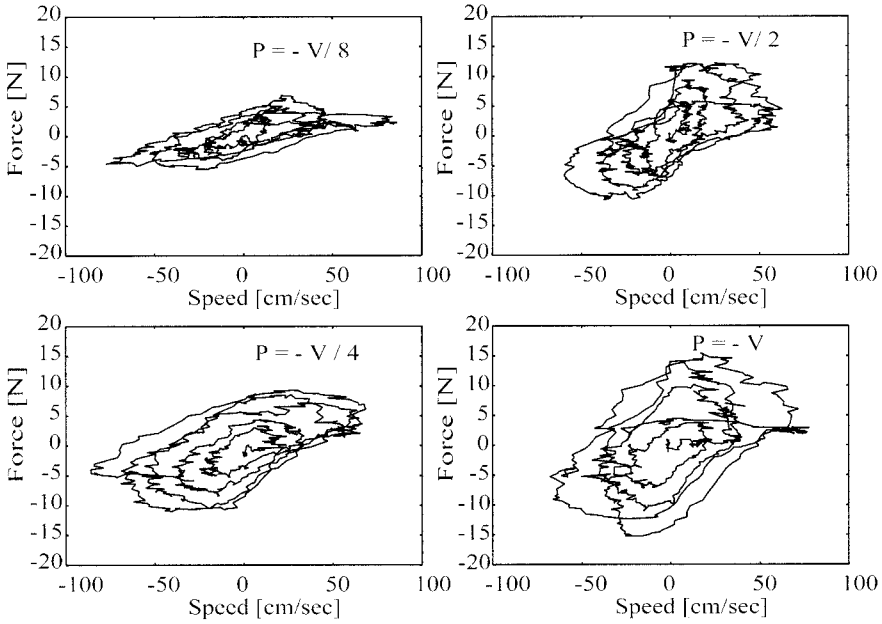

Figure 14. *Relation between speed and reaction force under four different vacuum pressure controls.*

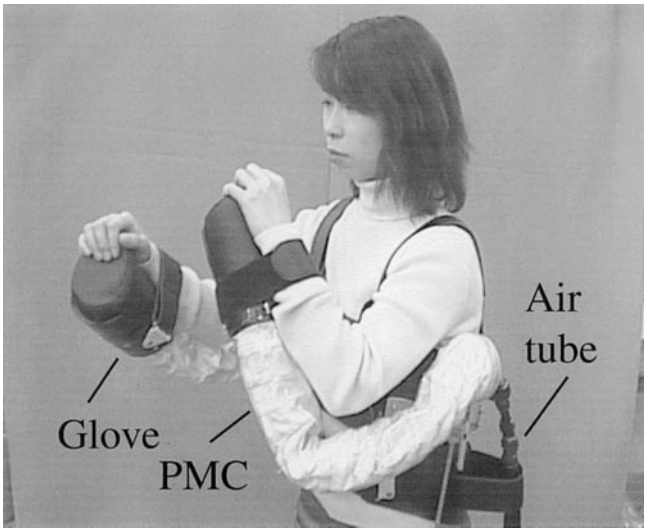

Figure 15. *A wearable haptic display.*

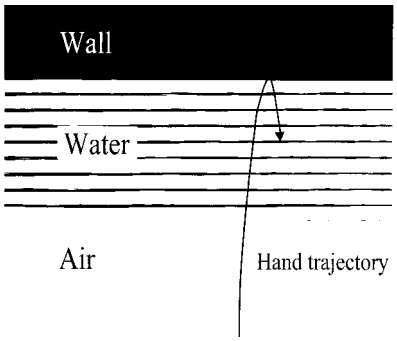

Figure 16. *Virtual haptic environment.*

softness, and safety. The operators showed no hesitation in wearing the PMC system, even though they felt a big reaction force when they touched the virtual wall. The plastic property of the PMC also contributes to the safety of the system; when the stiffness of the PMC was set to zero, hand motions such as twisting were not constrained at all. However, one demerit of this system is the limited degrees of freedom. For example, when the operator touches a virtual wall, this system constrains the position of the hand to provide a sensation of touching, but it also constrains the hand's ability to pull back from the wall. To solve this problem, the stiffness of the PMC was decreased when the system detected

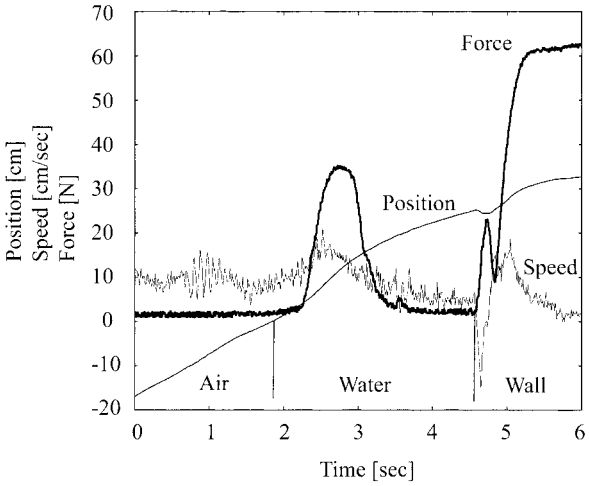

Figure 17. *Trajectories of hand position, hand speed, and reaction force.*

the hand pulling back, as in the experiment just described. However, it was impossible to provide a sensation of sliding the hand along the wall. To increase the degrees of freedom, multiple PMCs must be combined. This, too, remains as an interesting task in the development of the PMC.

6 Conclusions

In this study, we examined a novel mechanical element, called a *particle mechanical constraint,* whose stiffness can be controlled by vacuum pressure. By controlling the air pressure according to the deformation of the elements, the viscosity was also exerted. Because the PMC is lightweight and soft, it is suitable for use as a wearable human interface.

The main future development of this PMC is toward a reduction in the air capacity. Reducing the air capacity of the PMC may improve the reaction time for controlling the stiffness. Because the power of the vacuum pump and the size of the air tube are crucial to the reaction time, the current system uses a big vacuum pump and large tubes. The weight of the vacuum pump in the current system is 10 kg, which is too heavy to be worn comfortably. Because the pump is placed on the floor, the length of the air tube limits the mobility of the operator. To widen the fields of application for this wearable force display, it will be important to make the entire system smaller and lighter.

References

Aldridge, R. J., Carr, K., England, R., Meech, J. R., & Solomonides, T. (1996). Getting a grasp on virtual reality. *Proceedings of CHI 96,* 229–230.

Bergamasco, M., Allota, B., Bosio, L., Ferretti, L., Parrini, G., Prisco, G. M., Salsedo, F., & Sartini, G. (1994). An arm exoskeleton system for teleoperation and virtual environments applications. *Proceedings of the 1994 IEEE International Conference on Robotics and Automation,* 1449–1454.

Brooks, F. P., Young, M. O., Batter, J. J., & Kilpatrick, P. J. (1990). Project GROPE-Haptic display for scientific visualization. *Computer Graphics, 24*(4), 177–185.

Burdea, G., Zhuang, J., Roskos, E., Deborah, S., & Langrana, N. (1992). A portable dextrous master with force feedback. *Presence: Teleoperators and Virtual Environments, 1*(1), 18–28.

Colgate, J. E. (1996). Nonholonomic haptic display. *Proceedings of the 1996 IEEE International Conference on Robotics and Automation,* 539–544.

Ishii, M., & Sato, M. (1994). A 3D spatial interface device using tensed strings. *Presence: Teleoperators and Virtual Environments, 3*(1), 81–86.

Kawamura, S., Ida, M., Wada, T., & Wu, J. L. (1995). Development of a virtual sports machine using a wire drive system: A trial of virtual tennis. *Proceedings of the 1995 IEEE/RSJ International Conference on Intelligent Robots and Systems, 1,* 111–116.

Kazerooni, H., & Guo, J. (1993). Human extenders. *Journal of Dynamic Systems, Measurement, and Control, 115,* 281–290.

Sakaguchi, M., Fukusumi, K., & Furusho, J. (2000). Development and basic experiments of passive force display using ER brakes. *Proceedings of the 2000 Japan-USA Symposium on Flexible Automation,* CD-ROM.